IEEE Access
Multidisciplinary ⁝ Rapid Review ⁝ Open Access Journal

Received February 11, 2018, accepted March 18, 2018, date of publication March 29, 2018, date of current version April 23, 2018.

Digital Object Identifier 10.1109/ACCESS.2018.2820684

A Multiscale Autoregressive Model-Based Electrocardiogram Identification Method

JIKUI LIU[1], LIYAN YIN[1], CHENGUANG HE[1,2], BO WEN[1], XI HONG[1], AND YE LI[1], (Member, IEEE)

[1]Key Laboratory for Health Informatics, Shenzhen Institutes of Advanced Technology, Chinese Academy of Sciences, Shenzhen 518055, China
[2]Software School, North China University of Water Resources and Electric Power, Zhengzhou 450045, China

Corresponding author: Ye Li (ye.li@siat.ac.cn)

This work was supported in part by the National Natural Science Foundation of China under Grant 61771465, in part by the Science and Technology Planning of Guangdong Province under Grant 2017B030308007, in part by the Basic Research and Discipline Layout Project of Shenzhen under Grant JCYJ20170413161515911, Grant JCYJ20150630114942316, and Grant JSGG20160229123927512, and in part by the Special Program Foundation for Application of Guangdong Province under Grant 2015B010129012.

ABSTRACT With increasing security and privacy requirements, electrocardiogram (ECG)-based biometric human identification and authentication is gaining extensive attention. This paper aims to solve three major problems: stable identity feature is hard extracted from the inferior quality ECG, the performance of authentication system falls down when the size of registered sample set increases, and the authentication system needs to retrain when a new registered identity is added. To improve the robustness of identity feature, this paper proposed a multiscale feature extraction method using a multiscale autoregressive model (MSARM). First, the performance of multiscale feature was tested by simple matching method based on Chi-square distance in identification system. The test was performed on self-built SIAT-ECG and public PTB databases, which contain 146 and 100 (50 healthy volunteers and 50 patients with myocardial infarction) individuals, respectively. The recognition rate exceeded 93.15% for both databases in identification scenario. The results revealed that the MSARM has more excellent performance than other feature extraction methods. Then, this paper proposed a combination classifier method with one-to-one structure in authentication mode. It yielded a true rejection rate (TRR) of 98.99% and true acceptance rate (TAR) of 95.04% when registered sample set contains 140 individuals from SIAT-ECG database. Therefore, the proposed MSARM and combination classifier not only significantly improve the accuracy but also enhance the practicability of ECG-based biometric systems.

INDEX TERMS Combination classifiers, electrocardiogram identification, multiscale autoregressive model, random forest, template matching.

I. INTRODUCTION

With the development of information technology, information security concerns have become increasingly critical. Conventional identity verification tools such as credentials, secret keys and passwords can be easily copied and stolen. Thus they cannot meet the requirements of contemporary information security. Therefore, some secure biometrics technologies have been developed rapidly and applied gradually in recent years.

Various biometrics have been used in identity recognition, such as fingerprint, iris, face and speech. Although these biometrics systems have advantages such as a higher recognition rate, faster recognition speed and easier measurability, they have some disadvantages such as ease of replication and forgery [1]–[4]. In recent years, ECG signals have been used to resolve the human identification problem; these signals are a record of cardiac electrophysiological activity and reflect cardiac physiological functions [5]. Compared with common biometrics systems, ECG-based systems have unique advantages (TABLE 1). For example, ECG is pretty suitable for the healthcare scenario, since it is frequently monitored on patients. ECG signals can be measured only in a living body; therefore, they cannot be easily counterfeited. With the development of the ECG data-gathering technology, portable ECG signal-gathering devices, such as smart watches, have been designed in a highly convenient and intelligent manner. Therefore, ECG-based biometrics systems have broader applications.

TABLE 1. Performances comparison of biometrics character.

Biometrics	Accuracy	Security	Collectability	Cost
ECG	Medium	**High**	**High**	**Low**
Face	High	Low	High	Low
Iris	High	Medium	Medium	High
Fingerprint	High	Low	Medium	Medium
Voice Print	Low	Low	Low	Low

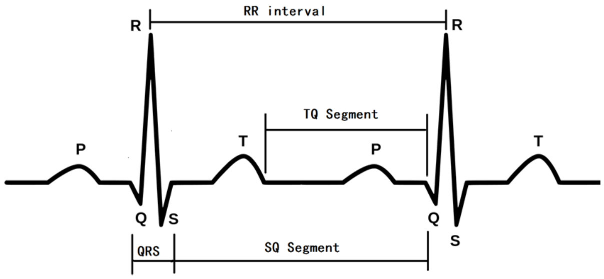

FIGURE 1. Characteristic points on ECG signals.

In recent years, studies have extensively explored ECG signals for use in identity recognition. These studies have mainly focused on different feature extraction methods, which can be divided into two main types: fiducial and nonfiducial detection. The fiducial detection method first detects the characteristic points of P, Q, R, S and T waves and then extracts the temporal features, amplitude, area, angle and dynamic features based on the fiducial points on ECG signals (Fig. 1). However, there is a weakness that the detection points need to be precise since a slightest variation of the fiducial point location may result in misclassifications[6]–[9]. By contrast, the nonfiducial detection method extracts discriminative information based on some nonlinear transformations from ECG signals without using characteristic points. Features such as autocorrelation, Fourier and wavelet coefficients are applied [10], [11]. Some studies have also proposed a composite method for extracting fiducial and nonfiducial features [12], [13].

Previous studies have described feature extraction methods based on one-channel, two-channel or multi-lead ECG signals, which were readily obtained from databases such as MIT-BIH and PTB. Some studies have demonstrated that only a single-lead ECG signal was adequate for identification. Shen et al. used template matching and a decision-based neural network (DBNN) as a classifier [7]. First, template matching was performed to compute correlation coefficients for comparing between two QRS complex waves. Next, a DBNN method was used to complete the verification from the possible identities IDs with the template matching. An accuracy rate of more than 95% may be achieved. Arteaga-Falconi et al. proposed time interval features based on fiducial points. The enrollment template was constructed by extracting eight features [15]. The following two aspects were considered subsequently in the process: the use of a feature-specific percentage of tolerance (i.e., each ECG feature has its own threshold) and the adoption of a hierarchical validation scheme, which yielded a false acceptance rate of 1.41% and a true acceptance rate (TAR) of 81.82% with 4 s of signal acquisition. Chan *et al.* [10] studied the classification performance of single-lead ECG data ; they used features which were based on the wavelet coefficients of lead I ECG signals from the MIT-BIH database and reported an accuracy of 90.4%. Zokaee and Faez [14] proposed a multimodal biometric identification system based on ECG signals and palm print analysis. They used the Mel-frequency cepstral coefficient approach to extract features from ECG signals; in addition, they performed principal component analysis to extract palm print features and achieved a recognition rate of 94.7%. Israel et al. [9] proposed an identification approach involving the use of 15 temporal features; they used Wilks' Lambda values for feature selection and linear discriminate analysis (LDA) for dimensionality reduction and classification, and they reported an identification accuracy of 90%. Some studies had also proposed new nonfiducial methods. For example, Lin *et al.* [15] selected the root mean square values, nonlinear Lyapunov exponent, and correlation dimensions to analyze ECG data after exercise and used a support vector machine (SVM) classifier to identify identity information; they achieved a recognition rate of more than 80%. Coutinho *et al.* [16] proposed a new nonfiducial ECG biometric identification method based on data compression techniques, namely the Ziv–Merhav cross parsing algorithm for symbol sequences (strings). This method depends on a string similarity measure derived from an algorithmic cross-complexity concept and its compression-based approximation; a recognition rate of 100% was achieved in 19 healthy individuals. Fatemain and Hatzinakos [17] developed a new wavelet-based framework for the automatic analysis of single-lead ECG signals for using in human recognition applications; they achieved an accuracy rate of 99.61% on PTB and MIT databases.

Although the methods proposed in the aforementioned studies have achieved high accuracy, these methods cannot be easily adopted to practical personal identification [1]. In summary, the aforementioned studies have the following limitations:

a) The proposed methods were developed on the basis of ECG signals of a diagnostic class. These ECG data have advantages such as low noise and working stability. Nevertheless, achieving high-quality ECG signals in daily applications is difficult.
b) Some studies on biometrics are based on 12-lead ECG data acquired from the MIT-BIH/PTB database. However, the acquisition of 12-lead ECG data is unrealistic in many situations or applications.
c) In most of the studies, the temporal interval of ECG records between the training and testing sets was very short or the records belonged to the same period, which was the primary contributor to higher recognition ratios. Notably, the accuracy rate remarkably

decreased for training and testing data obtained from different sessions.

In this study, an autoregressive model (ARM) was used to obtain power spectrum from ECG. The power spectrum of an ECG signal as an identity feature has better discriminative. To enhance the robustness of recognition features, a multiscale feature extraction method based on multiscale autoregressive model (MSARM) was proposed; in this method, the multiscale feature is a combination of power spectrum features on three scales with suitable weights, which is used to determine identity information. The results indicated that the proposed method exhibits satisfactory robustness for ECG signals of low quality or from myocardial infarction patients. In particular, the performance of the authentication system did not decrease significantly in a self-built ECG database from different sessions. In addition, this algorithm was determined to have a superior recognition ability compared with other algorithms on larger datasets. A typical human identification system is divided into identification and authentication modes. In the identification mode, the output of system can be used to identify an individual by using the input data. This mode requires only matching the most similar sample from the registered database. In the authentication mode, the system accepts or rejects an authentication request with the input data [1]. When the requested identity is wrongly rejected, the system incurs a false rejection error. Furthermore, when the requested identity is wrongly accepted, the system incurs a false acceptance error. In the present study, the realization schemes of the two aforementioned modes were designed: 1) for the identification mode, the system selects the most similar identity ID in the template library, serving as the recognition result of the input data. This selection can be achieved by template matching based on the distance (such as Euclidean, city block, chi-square and cosine distances). 2) The authentication mode involves a combination classifier composed of N parallel random forest sub-classifiers. The proposed authentication system does not require retraining of the entire system when registered individuals update, thus increasing the system's practicability. Moreover, the number of registered individuals does not affect the system's performance.

The rest of the paper was organized as follows. Section II describes the flow of the proposed identification system. Section III expounds the methods involved in preprocessing, feature extraction and classification steps. Section IV presents the analysis on the performance of the power spectrum feature and explains the experiment for the development of an optimal ARM. In Section V, we provide a comparison of the performance level of our method with those of other competitive algorithms on the SIAT-ECG and PTB databases. Finally, Section VI presents our study conclusions.

II. SYSTEM FLOW

Fig. 2 shows the flowchart of the identification/ authentication system. The first step involves the acquisition of raw ECG signals, which could be collected from three ECG electrodes placed on the wrist. The raw signals contain substantial noise and baseline drift part, which must be removed by using filters in the preprocessing step. Subsequently, features are extracted from the preprocessed ECG signals. This step is crucial for the performance of the system. In the model training step, the system is divided into identification and authentication modes, which conduct template building and model training, respectively. The final step of the system involves identity recognition, where the system outputs a matching result in the identification system and accepts or rejects in the authentication system. Each of these steps is described in detail in subsequent paragraphs.

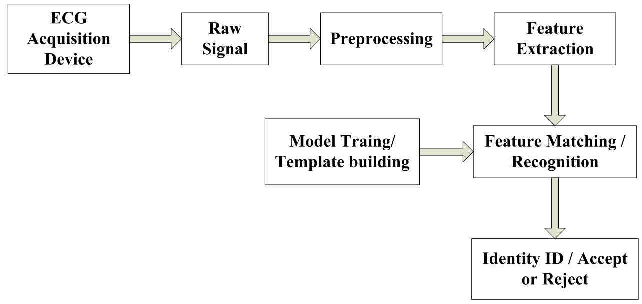

FIGURE 2. Flowchart of the identification system.

III. METHODS

A. PREPROCESSING

The electrical activity is transmitted through the chest, then signals are recorded on the skin surface; these signals are weak and have a low signal-to-noise ratio (SNR). The actual power of ECG signals is primarily concentrated in the 0.25–35 Hz range. The noise mainly includes power line (fixed 50 Hz in China), myoelectricity (5 Hz–2 KHz), electromagnetic interference and baseline wander (0.5–1 Hz). Noise interference is harmful for weak ECG signals because it severely corrupts the information of actual signals and directly affects the precision of feature extraction and classification processes. In particular, the interference becomes more severe for ECG signals acquired from wearable devices.

In this work, the ECG signal was acquired with a portable device on the wrist, which has lower SNR compared with standard 12-lead ECG. Therefore, noise removal is crucial for the entire system. In this study, denoising was performed in two stages: baseline wander removal and smoothing. A wavelet transform is suitable for multiscale analysis and can be used for multiresolution analysis in time and frequency domains. A baseline wander represents a low-frequency component of the signal, which can be separated from the original ECG signal through a wavelet transform. Subsequently, ECG signal smoothing was performed using the Butterworth low-pass filter with a 40 Hz cutoff frequency. Fig 3 presents the filtering results.

B. ARM-BASED FEATURE EXTRACTION METHOD

Feature extraction is one of the most crucial steps of an identity recognition system, and it directly affects the system's

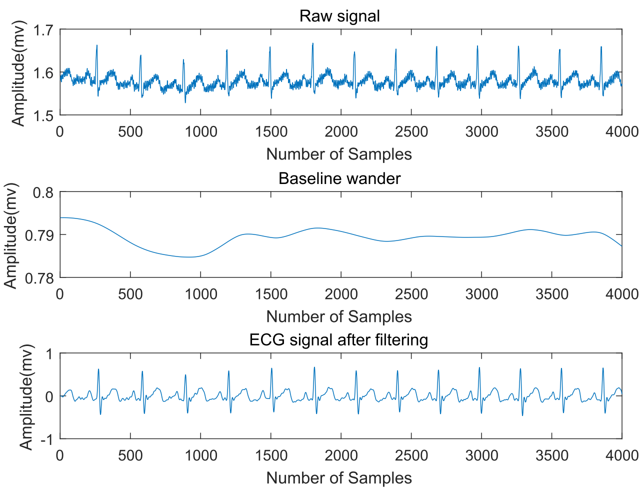

FIGURE 3. **ECG signal filtering results.**

performance. Features can be extracted from ECG signals by using two major methods: fiducial and nonfiducial detection. In the present study, a novel feature extraction method based on the nonfiducial detection was developed; the method uses an ARM to extract features from one ECG cycle between R peaks. The ARM is similar to the classical method (Fourier transform) that can be used to estimate the power spectrum of a signal. The unknown data outside the observation range is assumed to be zero in the classical spectrum estimation, which is equivalent to add window on the data. It results in reduction of resolution and stability of power spectra [18]. But the ARM power spectrum estimation does not have such imperfections, and it has obvious advantages both on the stability and resolution [19]–[22].

Assume that x (1), x (2)…x (n) represent the observation data of a stationary statistical process; the ARM can be represented by the following difference equation:

$$x(n) = -\sum_{k=1}^{p} a_k x(n-k) + w(n) \tag{1}$$

Where p represents the orders of the ARM, $a_k (k = 1, 2 \ldots p)$ represents the parameters of the p-order ARM, and $w(n)$ represents white-noise sequences with an average of 0 and variance of σ^2. The ARM is denoted as *AR (p)*. The $H(z)$ transition function of the ARM can be expressed as follows:

$$H(z) = \frac{X(z)}{W(z)} = \frac{1}{1 + \sum_{k=1}^{p} a_k z^{-k}} \tag{2}$$

For power spectrum estimation, assume that $x(n)$ represents the observation data of a stationary statistical process; the input $w(n)$ of the system is thus considered to be stable. Accordingly, the power spectrum of the observation data can be expressed as

$$p_x(\omega) = \sigma_w^2 \left| H(e^{j\omega}) \right|^2 = \frac{\sigma_w^2}{\left| 1 + \sum_{k=1}^{p} a_k e^{-jk\omega} \right|^2} \tag{3}$$

Equation (3) shows that the ARM can be used for power spectrum estimation, where the model parameters a_k and variance σ^2 of white-noise sequences must be determined. The autocorrelation function (ACF) of time series $x(n)$ can be expressed as

$$\begin{aligned} R_x(m) &= E\left\{x(n)x(n+m)\right\} \\ &= \begin{cases} -\sum_{k=1}^{p} a_k R_x(m-k) & m \geq 1 \\ -\sum_{k=1}^{p} a_k R_x(m-k) + \sigma^2 & m = 0 \end{cases} \end{aligned} \tag{4}$$

Then, (4) can be represented by the following matrix:

$$\begin{bmatrix} R_x(0) & R_x(1) & \cdots & R_x(p) \\ R_x(1) & R_x(0) & \cdots & R_x(p-1) \\ \vdots & \vdots & \vdots & \\ R_x(p) & R_x(p-1) & \cdots & R_x(0) \end{bmatrix} \begin{bmatrix} 1 \\ a_1 \\ \vdots \\ a_p \end{bmatrix} = \begin{bmatrix} \sigma^2 \\ 0 \\ \vdots \\ 0 \end{bmatrix} \tag{5}$$

Equation (5) is also referred to as the Yule–Walker equation. Therefore, the ARM parameters a_k and variance σ^2 can be obtained when the ACF of the observation data is known. One possible method for solving the Yule–Walker equation is the Burg algorithm, which does not require the direct calculation of the ARM parameter a_k. Instead, it calculates the reflection coefficient δ_i. The Burg algorithm uses the minimizing criterion of the total forward and backward predictive power errors to estimate reflection coefficients from the observational data. Moreover, the algorithm applies the recursive method to calculate the reflection coefficients. Specifically, the reflection coefficient δ_m in them^{th} step of the algorithm is calculated, and the coefficients $\delta_1 \ldots \delta_{m-1}$ remain constant. The reflection coefficient δ_1 can be calculated using (6), with $m = 1$ and initializing $e_0^f(n) = e_0^b(n) = x(n)$

$$\delta_m = \frac{-2\sum_{n=m}^{N-1} e_{m-1}^f(n) e_{m-1}^b(n-1)}{\sum_{n=m}^{N-1}\left[\left|e_{m-1}^f(n)\right|^2 + \left|e_{m-1}^b(n-1)\right|^2\right]} \tag{6}$$

Update equations (6), $e_m^f(n)$ and $e_m^b(n)$ can be calculated as follows:

$$e_m^f(n) = e_{m-1}^f(n) + \delta_m e_{m-1}^b(n-1)$$

$$e_m^b(n) = e_{m-1}^b(n-1) + \delta_m e_{m-1}^f(n)$$

The variables $e_m^f(n)$ and $e_m^b(n)$ are referred to as forward and backward prediction errors, respectively, which can be calculated using the next reflection coefficient δ_{m+1}. Equation (6) demonstrates that all reflection coefficients are guaranteed to have an absolute value of less than one. Finally, through the aforementioned iteration, the final reflection coefficient δ_p can be calculated. In addition, the parameter a_k of $ARM(p)$ can be solved by using the Levinson–Durbin equation.

Selecting an optimal ARM order is important for power spectrum estimation. A lower order results in decreasing precision of the power spectrum, whereas a higher order yields a false spectrum peak. The optimal model order can be estimated using the minimized order selection criterion. The Akaike information criterion (AIC) method is commonly used to select the optimal order. This method evaluates a given ARM by compromising both the linear predictive error and model complexity, which are based on information entropy. The optimal order is achieved at a lower AIC value. The AIC value is calculated as, $AIC = nln\,(RSS/n)$ where k is the ARM order, n is the length of the ECG cycle sequence, and $RSS = \sum_{j}^{n} \left(x_j - \hat{x}\right)$ where $\hat{x}$ and $\hat{x}$ are real-time and predictive time sequences, respectively. Furthermore, $nln\,(RSS/n)$ represents the performance of the predictive model, and $2k$ represents the complexity of the model for order k. A highly complex model usually results in an improved performance but also has an overfitting problem. The study computed the mean AIC values of different model orders in all training data and achieved an optimal order k at a lower AIC value.

C. MULTISCALE FEATURE EXTRACTION OF ECG SIGNALS

The multiscale analysis was widely applied in biomedical signal processing field [23]–[25]. The ECG signal contains P, QRS, T waves and resting period; the frequency feature is different in each ECG waves or period. It is typical biomedical signal that has obvious time-frequency and time-scale characteristics, thus the multiscale feature analysis for ECG signal is particularly suitable. A signal can be decomposed into different scales by multiscale analysis method. There are different time and frequency resolutions on different scales. Generally, a signal with high temporal resolution contains more detailed information, and a signal with low temporal resolution contains more global information. Therefore the signal can extract corresponding detailed and global features at different scales. These features are extremely suitable for using in identity recognition. For example, the global feature can reflect the discrepancy of overall ECG shape between different individuals; the detailed features can reflect detailed discrepancy. Thus these features fusion between different scales can improve the recognition rate of model.

As described in Section III-B, features can be extracted from a single ECG cycle by using the ARM. To exploit highly useful identity information from ECG signals for identification and authentication, a multiscale feature extraction method was developed. In this method, the features are extracted from the different scales of an ECG cycle by using the ARM; therefore, it is referred to as the multiscale ARM (MSARM). The wavelet transform is the most favorable tool for the multiscale analysis of ECG signals. Gaussian wavelet function has been used in decomposition of successive scales. The main reason for the selection of Gaussian wavelet function is its close similarity with the ECG signal. The ECG signal is segmented into different cardiac cycles by the R wave. Subsequently, the wavelet transform is applied to split the ECG signal into different scales (Fig. 4). With the layers calculated from top to bottom, the time resolution decreases, whereas the frequency resolution increases. The signal is split into approximation (cA) and detail (cD). The approximations in each level of cA1, cA2, and cA3 appear similar to original ECG signal approximations. The ECG signal contains various helpful identity features on different scales, which can improve the recognition accuracy. The present study used a three-level wavelet decomposition to obtain the features of the ECG signal based on the ARM. The three scales can be expressed as Sc1, Sc2, and Sc3. To extract features from the three scales, the features of each scale can be represented as ARM_1, ARM_2, and ARM_3, respectively. As shown in Fig.5, the power spectra distribution has significant differences on different scales, which are caused by different detailed and global information. The multiscale features are a weighted feature composition according to certain weights on different scales. The multiscale feature ARM can be expressed as $ARM = [\omega_1 * ARM_1, \omega_2 * ARM_2, \omega_3 * ARM_3]$, where ω_1, ω_2, and ω_3 are the weights of contribution, and $\omega_1 + \omega_2 + \omega_3 = 1$. The distinct contributions of the different scales are determined by computing the recognition rate rt_j for each scale. The weight can be set at $\omega_j = \frac{rt_j}{\sum_{j=1}^{3} rt_j}$. Fig. 6 illustrates the flowchart of the multiscale feature extraction method.

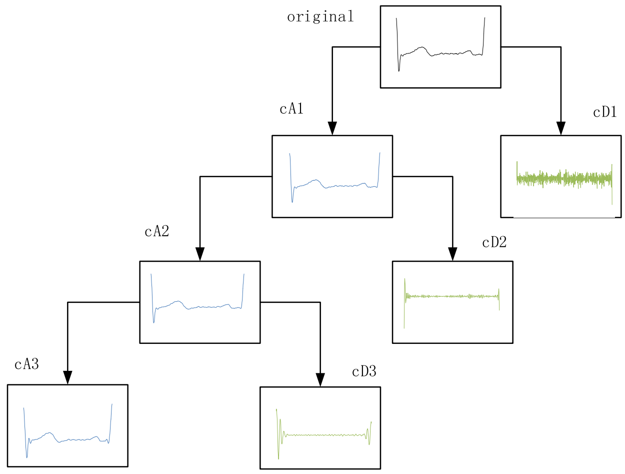

FIGURE 4. Three-level decomposition using the Gaussian wavelet function. cA1, cA2, and cA3 express the original approximation on each level, and cD1, cD2, and cD3 express the details on each level.

D. CLASSIFIER DESIGN

The final stage of the identity recognition system involves identification or authentication. Several common pattern recognition algorithms have been used in ECG signal-based identity recognition systems, including the k-nearest

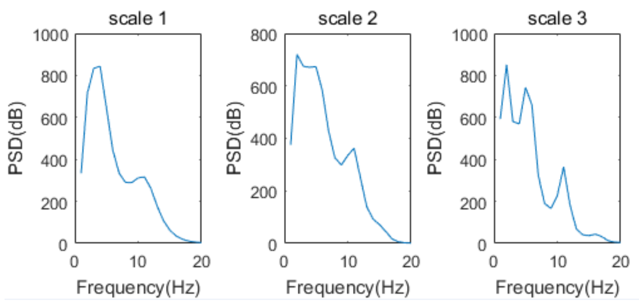

FIGURE 5. Power spectra of three-level ECG decomposition.

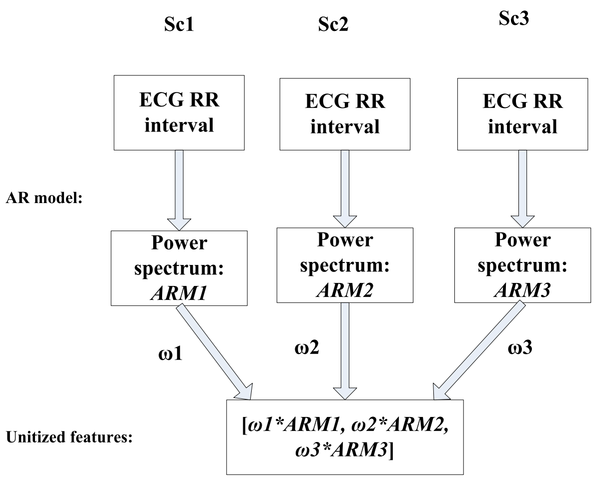

FIGURE 6. Flowchart of the multiscale feature extraction method.

neighbor [1], [11], [12], [26]–[29], SVM [30], [31], LDA [7], [9], [12], [31]–[34], nearest center [1], [10], [35]–[38], neural network [14], [39]–[42], generative model [11], [30], [43], [44] and multi-innovation identification method [45]–[48]. The identity recognition system proposed in the study is divided into one-to-many and many-to-one modes, which are used in the identification and authentication systems, respectively. In the one-to-many mode, the system selects the most similar identity ID in the training set as the recognition result of the input data. Furthermore, the template matching method is perfect for resolving the identification problem because it does not require a threshold. In addition, the method is simple and practical for identification because when registered individuals update, it only requires replacing the corresponding templates in the template library. This method identifies requested identity that are usually based on a correlation coefficient or the distance between the testing sample and target template. Several common algorithms of computed correlation and distance between the samples include the following: Pearson correlation coefficient, Spearman rank correlation, Euclidean distance, city block, Chi-square distance, and cosine distance. In the many-to-one mode, the system determines whether to accept or reject an authentication request from the input data. Therefore, an exact threshold is presented when the system uses the template matching method in authentication mode. However, obtaining an optimal threshold is very difficult, particularly for a larger authentication system.

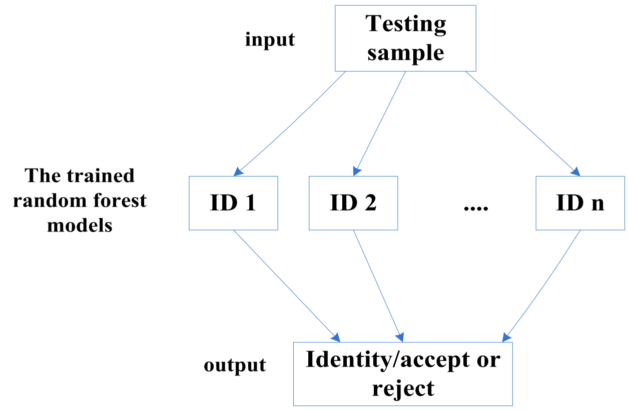

FIGURE 7. Random forest-based individualized verification framework. In the system, each identity has a random forest model in the training set. The output information is identified and either accepted or rejected.

To solve the aforementioned problem, we developed a random forest-based authentication system (Fig. 7). The system comprises input, multiple combination classifier, and output layers. The input layer involves the feature vector which is extracted from the ECG cycle by the proposed method. The combination classifier layer comprises N parallel random forest sub-classifiers. Random forest is a technique of supervised learning algorithm, which creates the forest with a number of trees. When the training set for the current tree is drawn by sampling with replacement, about one-third of the cases are left out of the sample. This out-of-bag data is used to get a running unbiased estimate of the classification error as trees are added to the forest. After each tree is built, all of the data are run down the tree, and proximities are computed for each pair of cases. If two cases occupy the same terminal node, their proximity is increased by one. At the end of the run, the proximities are normalized by dividing by the number of trees [49]. In this structure, one registered identity corresponds to one sub-classifier IDi from the combination classifier layer. All sub-classifiers can accept corresponding identity and reject other identities. Therefore, this combination classifier can be regarded as the one-to-one structure. For each sub-classifiers training, training samples are divided into two classes: positive samples and negative samples; the positive samples comprise 40 ECG cycles from the corresponding registered identity, and the negative samples comprise ECG cycles from other registered identities. Notably, once a sub-classifier was trained based on large training set, which can accept current registered identity and reject all unregistered identities, even the unregistered identity is not from the training set. The output is authentication information, which contains acceptance and rejection. The one-to-one multiple sub-classifier method can resolve two major concerns associated with the large authentication system: 1) the performance should not be influenced significantly when the system has many registered identities, and 2) training of the entire system is not required, only the corresponding sub-classifier model needs to be trained when a new registered identity is added

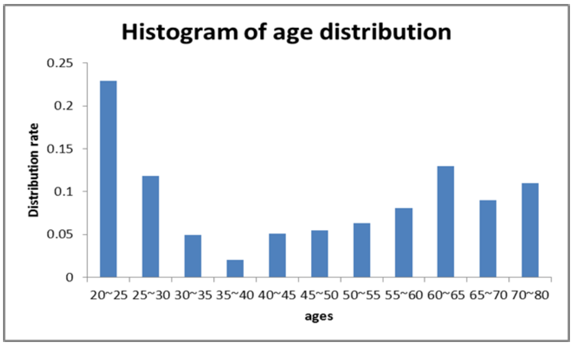

FIGURE 8. **Histogram of age distribution. In total, 146 subjects aged 20–80 years are included, and the male-to-female ratio is approximately 4:5.**

FIGURE 9. **Self-developed single-lead ECG signal acquisition device.**

into the system. This design has improved practicability and can be used in many application scenarios.

IV. EXPERIMENTS

A. SIAT-ECG DATABASE

The SIAT-ECG database was obtained from students and staff volunteers in Shenzhen Institutes of Advanced Technology (SIAT), Chinese Academy of Sciences, as well as from older volunteers in Lotus mountain communities in Shenzhen. The database includes information of 146 subjects, with the male-to-female ratio being about 4:5. Fig. 8 presents the age distribution. In this study, all ECG signals were single-lead signals collected from a self-developed portable device under a resting stage. The sampling frequency was 500 Hz (Fig. 9).

B. OBTAINING POWER SPECTRUM FEATURES OF ECG SIGNALS

We used the ARM to extract the power spectrum feature of an ECG cycle. In the experiment, the R peaks of the ECG cycles were detected on the basis of wavelet algorithms. Subsequently, each ECG cycle between two R peaks was extracted. Fig. 10 shows the power spectrum features extracted from an ECG cycle. The blue and red curves represent the power spectrum of training and testing sets from the same sample, respectively. In the present study, 40 continuous ECG

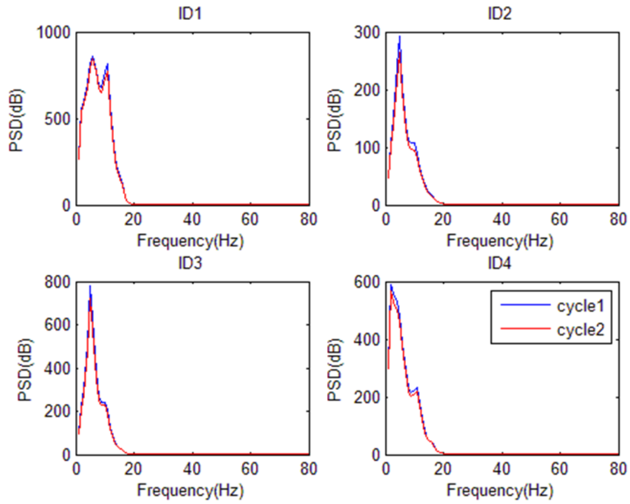

FIGURE 10. **Power spectrum of different ECG cycles from the same subject. ID1, ID2, ID3, and ID4 are four different subjects, where the red and blue curves represent the power spectrum of training and testing sets, respectively.**

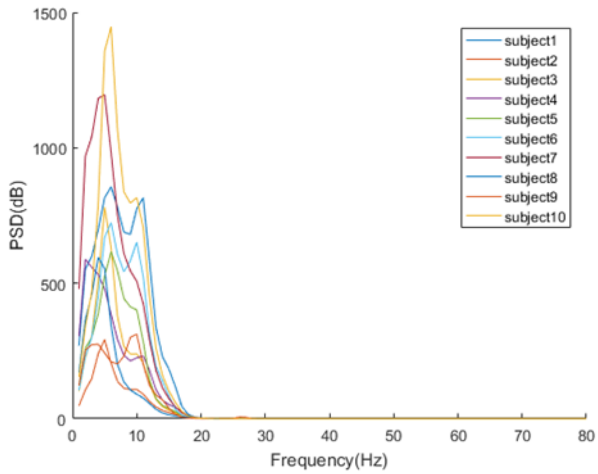

FIGURE 11. **Power spectra of ECG signals from different subjects.**

cycles were selected as candidate cycles of the registered identity. In identification mode, to reduce the disturbance from abnormal cycles, the K-means algorithm was used to eliminate 10 abnormal ECG cycles from candidate cycles. Finally, the average of all power spectrum feature vectors in the 30 normal cycles was used to set the matching template. Similarly, five continuous ECG cycles from other period of the same subject were used for test. As illustrated in Fig. 10, the estimated power spectra of different ECG cycles from the same subject were relatively similar. As shown in Fig. 11, the colored curves represent power spectra of ECG signals from different subjects. We can see that the power spectra have significant differences. Therefore, the power spectra of ECG signals are discriminative identity features because of their large inter-class distance and small intra-class distance.

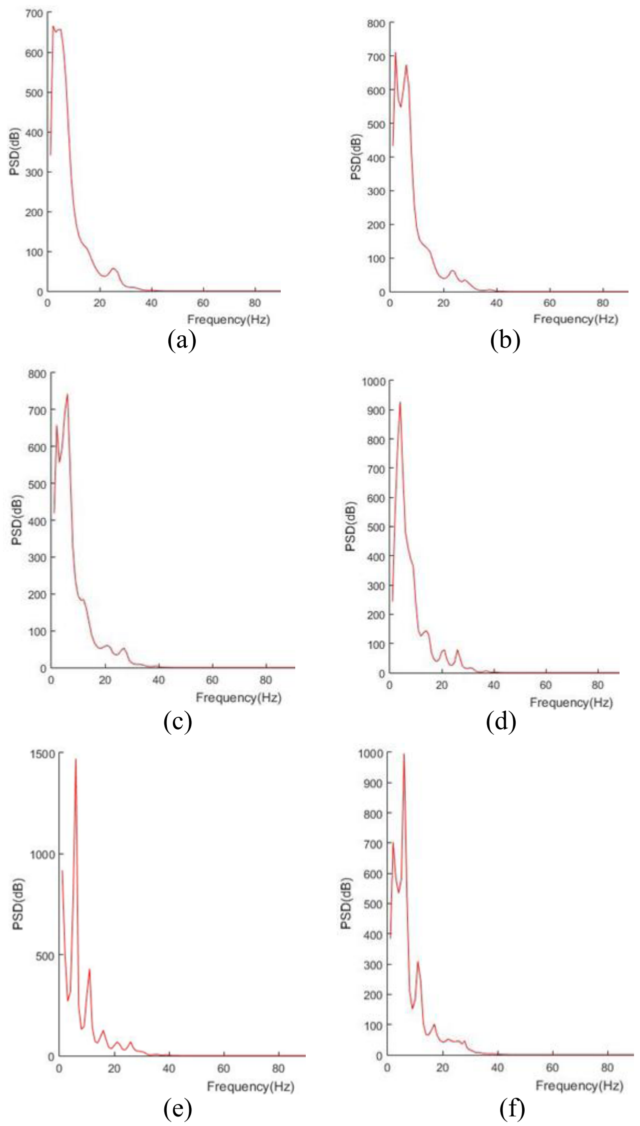

FIGURE 12. Power spectra at different ARM orders. (a)–(f) represent the power spectrum estimation of the orders 15, 20, 25... 40, respectively.

C. OPTIMIZING THE ARM ORDER

The ARM order directly affects the accuracy of power spectrum estimation. Therefore, the determination of an optimal ARM order is crucial. Fig. 12 shows the power spectrum estimation results derived at the orders 15, 20, 25... 40. Spurious peaks occurred frequently at orders of $p > 30$. By contrast, the power spectra were damped and smeared for lower orders ($p < 20$), which exhibited a lower precision. The AIC method to estimate the optimal ARM order was used. A lower AIC value implies an improved balance between prediction errors and model complexity. Although different individuals have different optimal model orders for their ECG signals, this study attempted to construct an ARM with the same order m for all subjects. The order m values ranging was explored from 5 to 40 to determine the optimal order associated with the lowest average AIC value. As shown in Fig. 13, the average minimum value was located at $p = 26$ for the AIC curve. The performance of the ARM markedly decreased at $p > 40$.

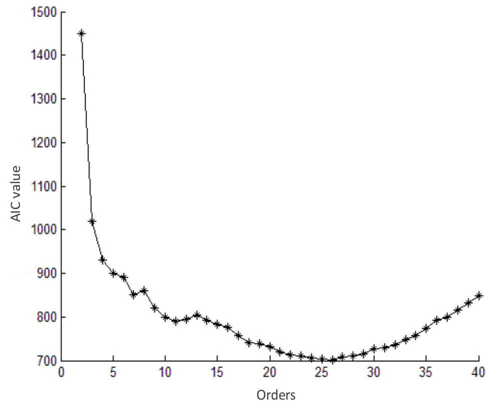

FIGURE 13. AIC values at different orders. The AIC value is minimum at $m = 26$.

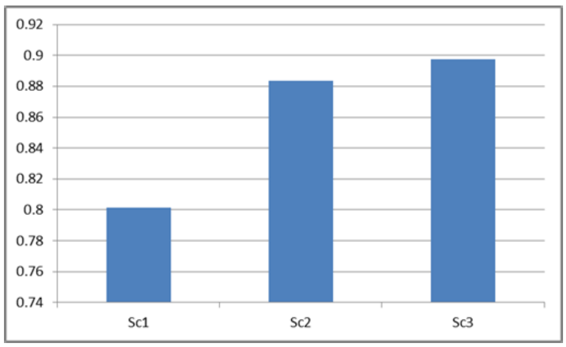

FIGURE 14. Recognition rate for the three scales based on the chi-square distance.

D. CALCULATING THE WEIGHTS OF CONTRIBUTION ON THREE SCALES

The weights of the contribution on different scales can be determined by computing the recognition rate on each scale. In general, discriminative features have a larger inter-class distance and a smaller intra-class distance. Therefore, we used a method based on distance discrimination to estimate the feature performance. Fig. 14 shows the recognition rates on three scales. The scales Sc1, Sc2, and Sc3 achieved accuracy rates of 80.14%, 88.36%, and 89.73%, respectively, for the SIAT-ECG database. Therefore, the weights of the contribution of the three scales were calculated using the formula $\omega_j = \frac{rt_j}{\sum_{j=1}^{3} rt_j}$. Sc1, Sc2, and Sc3 contributed weights of 0.3103, 0.3422, and 0.3475, respectively. Notably, weights would change for different databases so that they must be calculated separately.

V. RESULTS AND DISCUSSION

A. RESULTS OF IDENTIFICATION ON THE SIAT-ECG DATABASE

To evaluate the performance of the proposed method on databases with large samples and high-noise

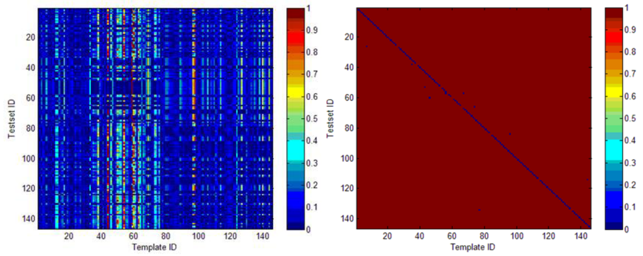

(a) (b)

FIGURE 15. Distance thermal mapping. (a) The thermal mapping of normalized distance data between 0 and 1 and (b) the thermal mapping of the identification results.

ECG signals, we used the SIAT-ECG database, which contains data of 146 individuals. The intra-class and inter-class can directly reflect the discrimination of features. For measurement of distance between samples, the chi-square has specific advantage compared with other methods, which can reflects relative relationship between the features better [50]. Therefore, we measured the similarity between two ECG signals based on chi-square distance, which is defined as follows: $\chi^2 = \sum \frac{(X-Y)^2}{Y}$, where $X = [x_1, x_2, \ldots, x_n]$ and $Y = [y_1, y_2, \ldots, y_n]$ represent the feature vectors of testing and registered samples, respectively. We examined the most similar power spectrum features between the testing samples and the template library. As shown in Fig.15, blue and red colors represent the greatest and the least similarities, respectively. Furthermore, to demonstrate the results effectively, we normalized the chi-square distances to the range [0, 1] [Fig. 15(a)]. Fig. 15(b) presents the binary results for Fig. 15(a), which is called binary thermal mapping. It clearly shows the matching results between the testing set and template library. For the 146 subjects in the testing set, nine were misidentified. The corresponding recognition rate was 93.15%. To demonstrate the robustness of our method on databases with large samples and high-noise ECG signals, we compared the recognition rate of our method with that of some competitive algorithms on the SIAT-ECG database (Table II). The result showed that the proposed method had great superiority to other methods. The recognition rate of other algorithms was up to 84.24%, which was substantially lower than those of the ARM (89.13%) and MSARM (93.15%). Furthermore, the recognition rate of the MSARM increased by 3.42% compared with that of the ARM. As illustrated in Fig. 16, most method achieved the recognition rates of more than 90%, except for the feature subspace ensemble method (FSE), when the template library had 20 subjects. However, the recognition accuracy decreased gradually with the increasing size of the template library. For example, the recognition rate of the proposed method decreased by 6.85% to 93.15% at a template size of 146. The recognition rates of competitive algorithms decreased by 8.41%–21.64%. This reduction may be caused by the increasing probability of similar samples with an expanding size of the template library. Thus, these results demonstrate that the proposed method exhibits superior robustness with respect to changes in the size of the template library, compared with other methods.

TABLE 2. comparison between the recognition rates of some competitive algorithms and our method on the SIAT-ECG database.

Method	Fiducial detection	Recognition rate
FSE	YES	65.06%
Wavelet Distance	NO	82.19%
Chaos Theory +BPNN	NO	84.24%
AR model + Template Matching	NO	89.73%
MSARM + Template Matching	NO	93.15%

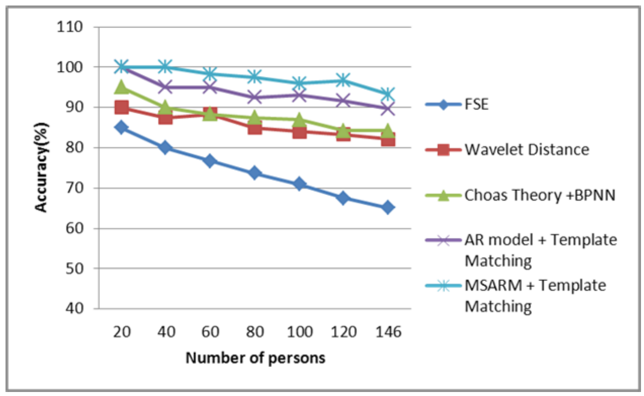

FIGURE 16. Recognition rates on subsets of different sizes from the SIAT-ECG database.

B. RESULTS OF IDENTIFICATION ON THE PTB DATABASE

To further evaluate the performance of the proposed method on a dataset of patients with myocardial infarction, we used the PTB database. This database contains 549 records obtained from 290 subjects (aged 17–87 years, mean age: 57.2 years). Each subject has one to five records, and each record contains 12 leads. The sampling frequency was 1000 Hz. The diagnostic classes of all subjects consisted of 148 patients with myocardial infarction, 52 healthy volunteers, and other classes. In this experiment, the performance was compared between patients with myocardial infarction and healthy volunteers. Therefore, 50 patients with myocardial infarction and 50 healthy volunteers were randomly selected from the PTB database. In addition, we selected lead I signals for ECG identification.

Fig. 17 shows the thermal mapping results obtained by applying the proposed method to the PTB database. Fig. 17(a) shows the thermal mapping results of 50 healthy volunteers. The experimental results revealed that 49 of 50 healthy volunteers were accurately identified, and only one volunteer was misidentified. The recognition rate was approximately 98%.

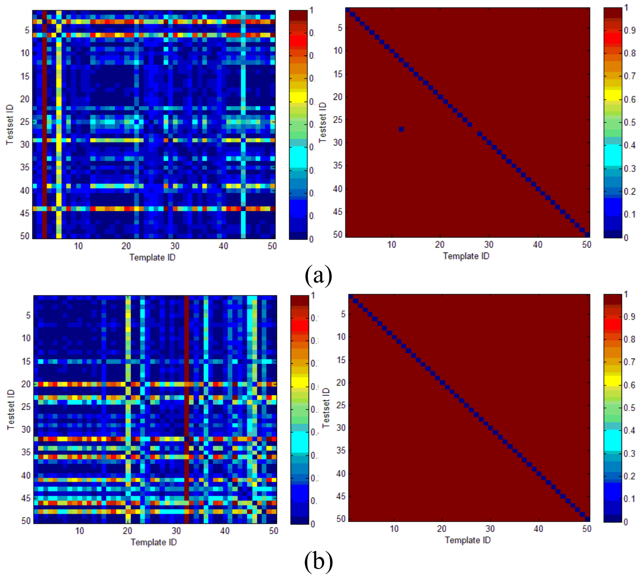

FIGURE 17. **Distance thermal mapping. (a) The thermal mapping results of healthy volunteers and (b) the thermal mapping results of patients with myocardial infarction.**

TABLE 3. **Comparison between the recognition rates of some competitive algorithms and our method on the datasets of healthy volunteers and patients with myocardial infarction from the PTB database.**

Method	Fiducial detection	Recognition rate(Health)	Recognition rate(MI)
FSE	YES	92%	76%
Wavelet Distance	NO	94%	82%
Chaos Theory +BPNN	NO	94%	86%
AR model +Template Matching	NO	96%	94%
MSARM +Template Matching	NO	98%	100%

The thermal mapping results of 50 patients with myocardial infarction were shown in Fig. 17(b). We can see that all patients with myocardial infarction were accurately identified. The recognition rate for patients with myocardial infarction does not decrease compared with that for healthy volunteers. We compared the proposed method with competitive algorithms in terms of their performance on the datasets of healthy volunteers and patients with myocardial infarction (Table 3). The performance levels of the ARM and MSARM were higher than those of other algorithms for the two datasets. The recognition rates of other algorithms were more than 92% for the healthy volunteer dataset; however, their recognition rates decreased significantly for the dataset of patients with myocardial infarction, and the minimum range decreased up to 8% with an accuracy of 86%. These results demonstrate that the proposed method has strong robustness and generalization compared with other algorithms.

C. RESULTS OF AUTHENTICATION ON THE SIAT-ECG DATABASE

We evaluated the authentication performance of the proposed method on the SIAT-ECG database. The evaluation indicators included the true rejection rate (*TRR*) and true acceptance rate (*TAR*). The true rejection is that sub-classifier can reject other identities which were defined as NS. The true acceptance is that the system can recognize correctly all registered identities which were defined as RS. A registered person may be accepted correctly or rejected erroneously, which is called a true acceptance sample (*TA*) or a false rejection sample (*FR*), respectively. The abbreviations denote the number of samples. Therefore, $RS = TA + FR$. Similarly, a nonregistered person may be rejected correctly or accepted erroneously, which is called a true rejection sample (*TR*) or a false acceptance samples (*FA*), respectively. Therefore, $NS = TR + FA$. The *TAR* is defined as $TAR = (TA/RS) * 100\%$, and the *TRR* is defined as $TRR = (TR/NS) * 100\%$.

We trained the random forest models for corresponding registered identities from the identified template library. This study proved that the random forest model with 25 trees can achieve the best performance. The red and blue curves in Fig. 18 represent the *TAR* and *TRR*, respectively. The horizontal axis indicates the number of individuals N in the training set. For each random forest sub-classifier, the training set consists of two subsets: 1) 40 ECG cycles from a registered identity corresponding to the sub-classifier as positive samples, and 2) $N - 1$ ECG cycles from the other $N - 1$ individuals as negative samples. In this study, the experiment was performed 10 times. From Fig.10, we can see that the *TRR* increased and the *TAR* decreased with the increasing size of the training set. For example, when the number of individuals in the training set was 140, the *TAR* and *TRR* were 99.25% and 94.62%, respectively. However, when the number of individuals increased to 130, the *TAR* and *TRR* were 95.04% and 98.99%, respectively. We believe that this phenomenon was caused by a higher number of negative samples in the training set, because only the number of negative samples increased with the increasing size of the training set. This represents a typical balance concern between positive samples and negative samples in the model training process. In many scenarios, this phenomenon can be useful. For example, when the system requires a higher security grade, the TRR must set to be higher (and vice versa).

For the sub-classifier, this study also compared the performance of common pattern algorithms with random forest as in TABLE 4. In the experiment, the size of the training set was 130. We can see random forest has the highest TRR. SVM can achieve TAR of 95.09% which is slightly higher than 95.04% of random forest-based model, but it only obtained TRR of 88.42%, which disadvantaged compared with other algorithms. Therefore, the sub-classifier with random forest has more excellent performance than other common pattern algorithms. Moreover, we can see that the sub-classifier used K- nearest neighboring also obtains a respectable performance. This further indicates two claims: the proposed

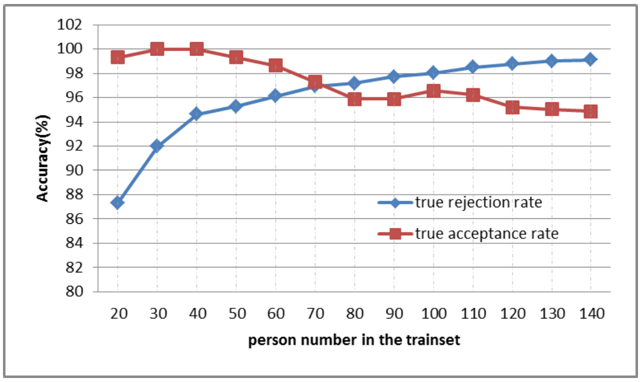

FIGURE 18. Result of verification on the training sets of different sizes. The red and blue curves represent the TAR and TRR of the testing samples, respectively.

TABLE 4. Comparison between the performance of some common pattern algorithms and random forest.

Method	*TRR*(%)	*TAR*(%)
Random forest	**98.99**	95.04
K- nearest neighboring	97.05	94.28
SVM	88.42	**95.09**
NaiveBayes	94.61	89.04
BP neural network	96.71	78.77

multiscale feature has excellent identity discrimination ability; the combination classifier with one-to-one mode also has certain universality.

VI. CONCLUSION

ECG-based biometric systems have distinctive advantages. For example, the inability of illegal individuals to deceive an ECG acquisition device in supervised scenarios is one of the reasons why such systems are an attractive alternative to other traditional biometric systems. This paper presents a novel MSARM-based feature extraction method for identification and authentication. In the identification experiments, a simple template matching method was used to evaluate the performance of the proposed method. The results indicate that the proposed method achieved a recognition rate of 93.15% and 100% on the SIAT-ECG and PTB (myocardial infarction group) database, respectively. The following inferences can be derived from the evaluation results of the two databases: 1) The proposed method exhibited satisfactory robustness for ECG signals of low quality or from cardiac patients and 2) the extracted features were discriminative because of their small intra-class distance and large inter-class distance. Furthermore, we compared the performance of the MSARM and ARM feature extraction methods, and the results indicate that multiscale information extraction is necessary for effective feature discrimination.

To enhance the practicability of ECG-based biometric systems, we further used a combination classifier based on random forest to verify the identity request. The designed one-to-one structure in combination classifier mainly avoids retraining the entire authentication system when the registered members update. This design is very useful for practical applications and can effectively avoid deteriorations of system performance caused by considerable increase of registered members. The experimental results show that both *TAR* and *TRR* achieved more than 95% on the SIAT-ECG database. Furthermore, the system performance only decreased slightly with the increasing number of registered members. Therefore, this design is very effective for practical applications.

Although the proposed method yielded the most favorable results among all compared methods, some unavoidable questions remain; for example, ECG signals were collected under the resting state in all previous studies. However, ECG signals may fluctuate under different states or moods. The performance level of our method was evaluated in large groups of 146 subjects and was compared with those of other methods. Nevertheless, its reliability should be evaluated in even larger groups. Currently, larger ECG databases with diverse activity and emotional states are not available. We desire to develop such ECG databases in our future studies to obtain a comprehensive understanding of ECG-based biometric systems.

ACKNOWLEDGMENT

The experimental place and equipment were provided by the CAS Key Laboratory of Health Informatics and Shenzhen Engineering Laboratory of Health Big Data. The authors would like to thank the three anonymous reviewers for their detailed comments, corrections and to improve the quality of this paper. The authors would also like to thank the open PTB database for supplying the ECG data.

REFERENCES

[1] I. Odinaka, P.-H. Lai, A. D. Kaplan, and J. A. O'Sullivan, E. J. Sirevaag, and J. W. Rohrbaugh, "ECG biometric recognition: A comparative analysis," *IEEE Trans. Inf. Forensics Security*, vol. 7, no. 6, pp. 1812–1824, Dec. 2012.

[2] R. M. Bolle, J. Connell, S. Pankanti, N. K. Ratha, and A. W. Senior, *Guide to Biometrics*. Springer, 2013.

[3] D. Menotti *et al.*, "Deep representations for iris, face, and fingerprint spoofing detection," *IEEE Trans. Inf. Forensics Security*, vol. 10, no. 4, pp. 864–879, Apr. 2015.

[4] J. Chirillo and S. Blaul, *Implementing Biometric Security*. New York, NY, USA: Hungry Minds, Incorporated, 2003.

[5] A. D. C. Chan, M. M. Hamdy, A. Badre, and V. Badee, "Person identification using electrocardiograms," in *Proc. Can. Conf. Elect. Comput. Eng.*, May 2006, pp. 1–4.

[6] L. Biel, O. Pettersson, L. Philipson, and P. Wide, "ECG analysis: A new approach in human identification," *IEEE Trans. Instrum. Meas.*, vol. 50, no. 3, pp. 808–812, Jun. 2001.

[7] M. Kyoso and A. Uchiyama, "Development of an ECG identification system," in *Proc. 23rd Annu. Int. Conf. IEEE Eng. Med. Biol. Soc.*, vols. 1–4. Oct. 2001, pp. 3721–3723.

[8] T. W. Shen, W. J. Tompkins, and Y. H. Hu, "One-lead ECG for identity verification −2(nd) joint conference of the IEEE engineering in medicine and biology society and the biomedical engineering society," in *Proc. 2nd Joint EMBS-BMES Conf.*, vols. 1–3. 2002, pp. 62–63.

[9] S. A. Israel, J. M. Irvine, A. Cheng, M. D. Wiederhold, and B. K. Wiederhold, "ECG to identify individuals," *Pattern Recognit.*, vol. 38, no. 1, pp. 133–142, Jan. 2005.

[10] A. D. C. Chan, M. M. Hamdy, A. Badre, and V. Badee, "Wavelet distance measure for person identification using electrocardiograms," *IEEE Trans. Instrum. Meas.*, vol. 57, no. 2, pp. 248–253, Feb. 2008.

[11] K. N. Plataniotis, D. Hatzinakos, and J. K. M. Lee, "ECG biometric recognition without fiducial detection," in *Proc. Biometrics Symp., Special Session Res. Biometric Consortium Conf.*, Aug. 2006, pp. 1–6.

[12] Y. J. Wang, F. Agrafioti, D. Hatzinakos, and K. N. Plataniotis, "Analysis of human electrocardiogram for biometric recognition," *EURASIP J. Adv. Signal Process.*, vol. 2008, Dec. 2007, Art. no. 148658.

[13] H. Silva, H. Gamboa, and A. Fred, "One lead ECG based personal identification with feature subspace ensembles," in *Proc. Int. Workshop Mach. Learn. Data Mining Pattern Recognit.*, Jul. 2007, pp. 770–783.

[14] S. Zokaee and K. Faez, "Human identification based on ECG and palmprint," *Int. J. Elect. Comput. Eng.*, vol. 2, no. 2, p. 261, 2012.

[15] S.-L. Lin, C.-K. Chen, C.-L. Lin, W.-C. Yang, and C.-T. Chiang, "Individual identification based on chaotic electrocardiogram signals during muscular exercise," *IET Biometrics*, vol. 3, no. 4, pp. 257–266, Dec. 2014.

[16] D. P. Coutinho, A. L. N. Fred, and M. A. T. Figueiredo, "One-lead ECG-based personal identification using Ziv–Merhav cross parsing," in *Proc. 20th Int. Conf. Pattern Recognit. (ICPR)*, Aug. 2010, pp. 3858–3861.

[17] S. Z. Fatemian and D. Hatzinakos, "A new ECG feature extractor for biometric recognition," in *Proc. 16th Int. Conf. Digit. Signal Process.*, vols. 1–2, Jul. 2009, pp. 323–328.

[18] B. M. Kay, *Modern Spectral Estimation: Theory and Application*. Englewood Cliffs, NJ, USA: Prentice-Hall, 1988.

[19] H. He, X. Huang, F. Liu, D. J. Zhang, and M. F. Hou, "The simulation of burg algorithm for AR model power spectrum estimation," *Mater. Sci. Eng.*, vols. 179–180, pp. 426–430, Jan. 2011.

[20] T. Al-Ani, F. Cazettes, S. Palfi, and J.-P. Lefaucheur, "Automatic removal of high-amplitude stimulus artefact from neuronal signal recorded in the subthalamic nucleus," *J. Neurosci. Methods*, vol. 198, no. 1, pp. 135–146, May 2011.

[21] M. D. Ortigueira and J. M. Tribolet, "Global versus local minimization in least-squares AR spectral estimation," *Signal Process.*, vol. 7, no. 3, pp. 267–281, Dec. 1984.

[22] J. B. Tary, R. H. Herrera, and M. van der Baan, "Time-varying autoregressive model for spectral analysis of microseismic experiments and long-period volcanic events," *Geophys. J. Int.*, vol. 196, no. 1, pp. 600–611, Jan. 2014.

[23] T. Nakamura, K. Kiyono, H. Wendt, P. Abry, and Y. Yamamoto, "Multiscale analysis of intensive longitudinal biomedical signals and its clinical applications," *Proc. IEEE*, vol. 104, no. 2, pp. 242–261, Feb. 2017.

[24] X. Shen and A. I. Zayed, Eds., *Multiscale Signal Analysis and Modeling*. New York, NY, USA: Springer, 2013.

[25] A. Meyer-Bäse and F. J. Theis, *Biomedical Signal Analysis*. Cambridge, MA, USA: MIT Press, 2010.

[26] F. Agrafioti and D. Hatzinakos, "ECG biometric analysis in cardiac irregularity conditions," *Signal Image Video Process.*, vol. 3, pp. 329–343, Dec. 2009.

[27] M. Homer, J. M. Irvine, and S. Wendelken, "A model-based approach to human identification using ECG," *Proc. SPIE*, vol. 7306, p. 730625, May 2009.

[28] N. Ghofrani and R. Bostani, "Reliable features for an ECG-based biometric system," in *Proc. 17th Iranian Conf. Biomed. Eng. (ICBME)*, Nov. 2010, pp. 1–5.

[29] M. Li and S. Narayanan, "Robust ECG biometrics by fusing temporal and cepstral information," in *Proc. 20th Int. Conf. Pattern Recognit. (ICPR)*, Aug. 2010, pp. 1326–1329.

[30] C. Ye, M. T. Coimbra, and B. V. K. Vijaya Kumar, "Investigation of human identification using two-lead electrocardiogram (ECG) signals," in *Proc. 4th IEEE Int. Conf. Biometrics, Theory Appl. Syst. (BTAS)*, Sep. 2010, pp. 1–8.

[31] T.-W. Shen, W. J. Tompkins, and Y. H. Hu, "Implementation of a one-lead ECG human identification system on a normal population," *J. Eng. Comput. Innov.*, vol. 2, no. 1, pp. 12–21, 2011.

[32] K.-S. Kim, T.-H. Yoon, J.-W. Lee, D.-J. Kim, and H.-S. Koo, "A robust human identification by normalized time-domain features of electrocardiogram," in *Proc. 27th Annu. Int. Conf. Eng. Med. Biol. Soc. (IEEE-EMBS)*, Jan. 2006, pp. 1114–1117.

[33] M. Kyoso, "A technique for avoiding false acceptance in ECG identification," in *Proc. IEEE EMBS Asian–Pacific Conf. Biomed. Eng.*, Oct. 2003, pp. 190–191.

[34] G. Wübbeler, M. Stavridis, D. Kreiseler, R.-D. Bousseljot, and C. Elster, "Verification of humans using the electrocardiogram," *Pattern Recognit. Lett.*, vol. 28, no. 10, pp. 1172–1175, Jul. 2007.

[35] G. G. Molina, F. Bruekers, C. Presura, M. Damstra, and M. van der Veen, "Morphological synthesis of ECG signals for person authentication," in *Proc. 15th Eur. Signal Process. Conf.*, Sep. 2007, pp. 738–742.

[36] C.-C. Chiu, C.-M. Chuang, and C.-Y. Hsu, "A novel personal identity verification approach using a discrete wavelet transform of the ECG signal," in *Proc. Int. Conf. Multimedia Ubiquitous Eng. (MUE)*, Apr. 2008, pp. 201–206.

[37] J. M. Irvine, S. A. Israel, W. T. Scruggs, and W. J. Worek, "eigenPulse: Robust human identification from cardiovascular function," *Pattern Recognit.*, vol. 41, no. 11, pp. 3427–3435, Nov. 2008.

[38] B. Anuradha and V. C. V. Reddy, "ANN for classification of cardiac arrhythmias," *ARPN J. Eng. Appl. Sci.*, vol. 3, no. 3, pp. 1–6, Jun. 2008.

[39] J. C. Loong, K. S. Subari, R. Besar, and M. K. Abdullah, "A new approach to ECG biometric systems: A comparative study between LPC and WPD systems," in *Proc. World Academy Sci., Eng. Technol.*, vol. 68. 2010, pp. 759–764.

[40] Y. Wan and J. Yao, "A neural network to identify human subjects with electrocardiogram signals," in *Proc. World Congr. Eng. Comput. Sci. (WCECS)*, 2008, pp. 13–16.

[41] R. Palaniappan and S. M. Krishnan, "Identifying individuals using ECG beats," in *Proc. Int. Conf. Signal Process. Commun. (SPCOM)*, Dec. 2004, pp. 569–572.

[42] J. M. Irvine and S. A. Israel, "A sequential procedure for individual identity verification using ECG," *EURASIP J. Adv. Signal Process.*, vol. 2009, Dec. 2009, Art. no. 243215.

[43] I. Odinaka *et al.*, "ECG biometrics: A robust short-time frequency analysis," in *Proc. IEEE Int. Workshop Inf. Forensics Secur. (WIFS)*, Dec. 2010, pp. 1–6.

[44] F. Ding, X. Wang, L. Mao, and L. Xu, "Joint state and multi-innovation parameter estimation for time-delay linear systems and its convergence based on the Kalman filtering," *Digit. Signal Process.*, vol. 62, pp. 211–223, Mar. 2017.

[45] X. Wang, F. Ding, T. Hayat, and A. Alsaedi, "Combined state and multi-innovation parameter estimation for an input non-linear state-space system using the key term separation," *IET Control Theory Appl.*, vol. 10, no. 13, pp. 1503–1512, Aug. 2016.

[46] F. Ding, *Several Multi-Innovation Identification Methods*. New York, NY, USA: Academic, 2010.

[47] F. Ding, P. X. Liu, and G. Liu, "Multiinnovation least-squares identification for system modeling," *IEEE Trans. Syst., Man, Cybern. B, Cybern.*, vol. 40, no. 3, pp. 767–778, Jun. 2010.

[48] L. Breiman, "Random forests," *Mach. Learn.*, vol. 45, no. 1, pp. 5–32, Oct. 2001.

[49] "Chi-square distance," in *The Concise Encyclopedia of Statistics*. New York, NY, USA: Springer, 2008, pp. 68–70.

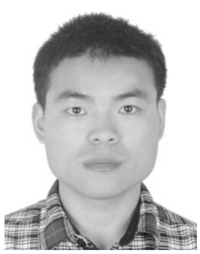

JIKUI LIU received the B.S. degree in biomedical engineering from Taishan Medical University, Tai'an, China, in 2010, and the M.S. degree from the Changchun University of Science and Technology, Changchun, China, in 2013. Since 2013, he has been a Research Associate with the Research Center for Biomedical Information Technology, Shenzhen Institutes of Advanced Technology, Chinese Academy of Sciences. His main research interests include biomedical signal processing, biometrics, and machine learning.

LIYAN YIN received the B.S. degree in food engineering, the M.S. degree in food engineering, and the Ph.D. degree in agricultural electrification and automation from Jilin University, Changchun, China, in 2004, 2007, and 2011, respectively. Since 2010, she has been an Engineer of Shenzhen Biocare Bio-Medical Equipment Co., Ltd. Since 2015, she has been an Engineer of the Research Center for Biomedical Information Technology, Shenzhen Institutes of Advanced Technology. Her current research interests include biomedical signal processing and wearable devices.

CHENGUANG HE received the B.S. in software theory from Henan Normal University in 1996, the M.S. degrees in software theory from Yunnan University in 2008, and the Ph.D. degree in computer application technology from the Shenzhen Institutes of Advanced Technology, Chinese Academy of Sciences in 2015. He is currently an Associate Professor with the North China University of Water Resources and Electric Power. His research interests include the security of cloud computing and applications of Internet of Things.

BO WEN received the B.S. degree from the Huazhong University of Science and Technology, Wuhan, China, in 2015. He is currently pursuing the master's degree with the Research Center for Biomedical Information Technology, Shenzhen Institutes of Advanced Technology, Chinese Academy of Sciences. His research field includes wearable computation.

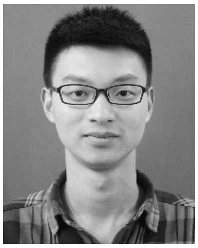

XI HONG received the B.S. and M.S. degrees from the Huazhong University of Science and Technology, Wuhan, China, in 2014 and 2017, respectively. Since 2015, he has been an intern with the Research Center for Biomedical Information Technology, Shenzhen Institutes of Advanced Technology, Chinese Academy of Sciences. His research field includes feature points detection of biological signal and machine learning.

YE LI received the B.S. and M.S. degrees from the University of Electronic Science and Technology of China, Chengdu, China, in 1999 and 2002, respectively, and the Ph.D. degree from Arizona State University, Tempe, AZ, USA, in 2006, all in electrical engineering. Since 2008, he has been the Director of the Research Center for Biomedical Information Technology, Shenzhen Institutes of Advanced Technology, where he is currently a Professor with the Chinese Academy of Sciences. His current research interests include wireless body sensor networks, wearable devices, and mobile health.